Evidence for small-scale plasma irregularities at mid-latitudes: Introduction and validation of large-scale GPS scintillation imaging

Sebastijan Mrak[1], Joshua Semeter[1], Toshi Nishimura[1]

[1]Department of Electrical and Computer Engineering and Center for Space Physics, Boston University

Introduction

Signals from global navigation systems are commonly used diagnostic for ionospheric plasma dynamics. In particular, high frequency fluctuations (scintillation) of received amplitude, and phase are a handy diagnostic for small-scale (~100m to ~km) size irregularities. Dedicated scintillation receivers are utilized for such purposes, however, they are predominantly operated at low and high latitudes. **Our goal is to survey the mid-latitudes with scintillation occurrence with high-rate geodetic receivers.** We define mid-latitudes as the region of magnetic latitude 30 <= MLAT <= 60.

We present the first large-scale Global Positioning System (GPS) scintillation imaging product, leveraging the UNAVCO geodetic GPS receivers. While dealing with large verity of hardware, we introduce the receiver and time dependent processing, together with modified scintillation indices. Spatial distribution of the receivers enable the first comprehensive study of the mid-latitude ionosphere, with ~400 receivers the North American sector. We find that the mid-latitudes host storm-time small-scale irregularities, which are independently validated by in-situ electron density measurements by the SWARM spacecraft.

Methodology

The receiver limitations prevent us from using of conventional phase (σ_φ), and amplitude (S_4) scintillation indices. Nevertheless, we choose to define their proxy indices σ_{TEC} and SNR_4, respectively. We utilize Total Electron Content (TEC) as an indicator for phase fluctuations, and Signal to Noise Ratio (SNR) as a substitute for amplitude. The new definitions follow the standard morphology:

$$\sigma_{TEC} = \sqrt{<TEC^2> - <TEC>^2}$$

$$SNR4 = \sqrt{<SNR^2> - <SNR>^2}$$

The indices are defined as a standard deviation of respective parameter for a time period of 60 seconds. Each index is computed in three steps, depicted in Figure 1 for σ_{TEC}; (1) Polynomial de-trending (ΔTEC). (2) High-pass filtering, 6th order Butterworth filter, 0.1 Hz (δTEC). (3) Moving standard deviation filter (σ_{TEC}, SNR_4).

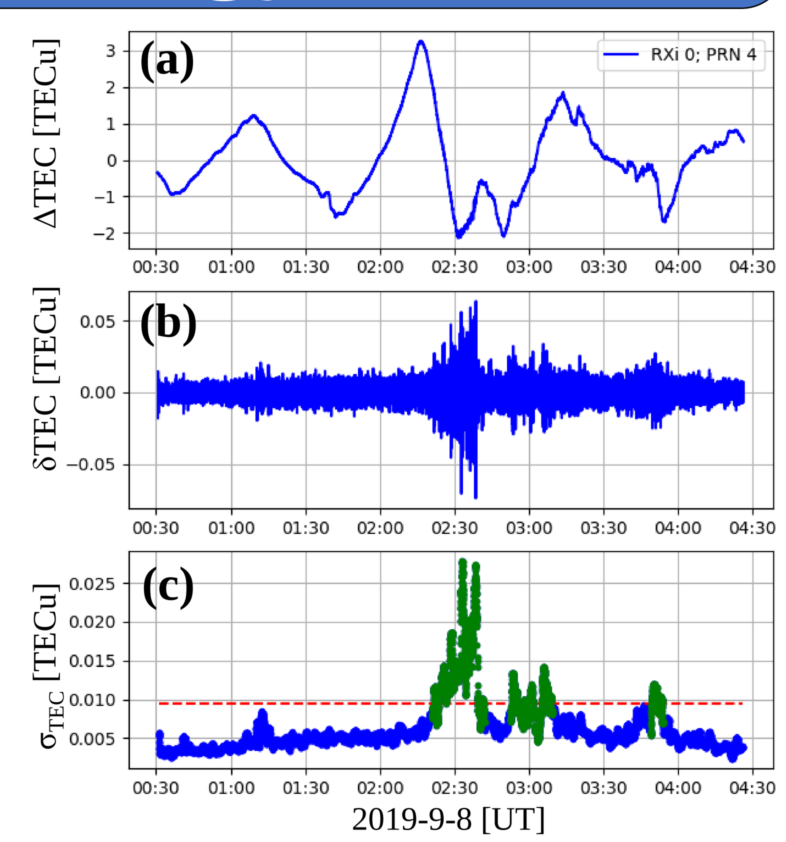

Figure 1: Demonstration of the three-step scintillation index/event processing for σ_{TEC}. Red dashed line the E-limit, green samples represent instances of scintillation events.

All receivers have a temporal resolution of 1 Hz, therefore, the artificial cutoff at 0.1 Hz is a band-pass filter for irregularities at temporal scales between 2 – 10 seconds. However, there is inherent space-time ambiguity due to non-stationary plasma.

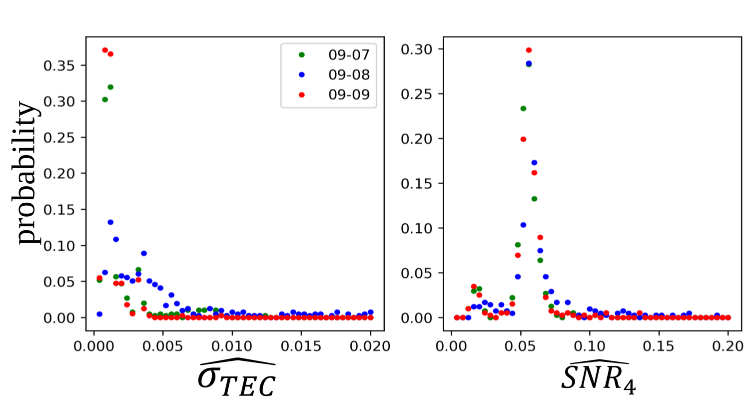

Figure 2: Histogram of a median standard deviations for TEC and SNR encompassing ~420 receivers for 3 days in September 2017.

A use of large verity of hardware comes at a cost of in general larger receiver varaince, use of proxy indices, and additional processing routines to mitigate outliers. In order to mitigate receiver-time-dependent background noise, we define a scintillation event as:

A continuous time period when a scintillation index exceeds a value $E = 2 \cdot \widehat{\sigma_{TEC}}$, where $\widehat{\sigma_{TEC}}$ is a median value of the scintillation index for a receiver per day. Same for the SNR_4. An event extraction is demonstrated in Figure 1c, where red dashed line a value of **E**, and green samples were determent as scintillation events.

Large spread in receiver hardware performance is demonstrated in Figure 2, where a distribution of median values of σ_{TEC} and SNR4 is evaluated for 420 receivers, in three consecutive days. Median σ_{TEC} is 0.12 TECu/s, which is an order of magnitude larger from scintillation receivers.

Scintillation Imaging

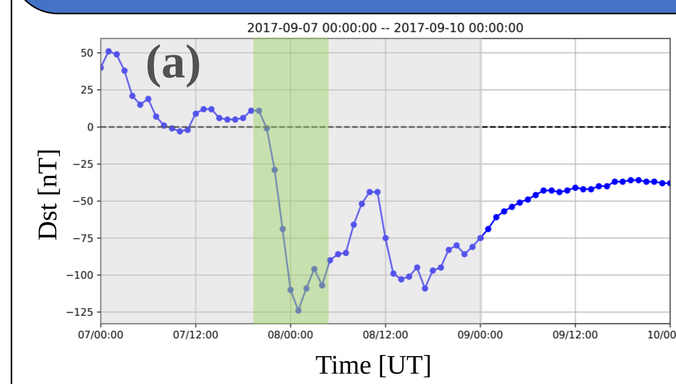

Figure 3: (a) Dst index for the time period of interest. (b) Map of the GPS receivers. Overall 423 receivers, ~320 of them are located at mid-latitudes (red dots). Others are at low and high latitude (white dots).

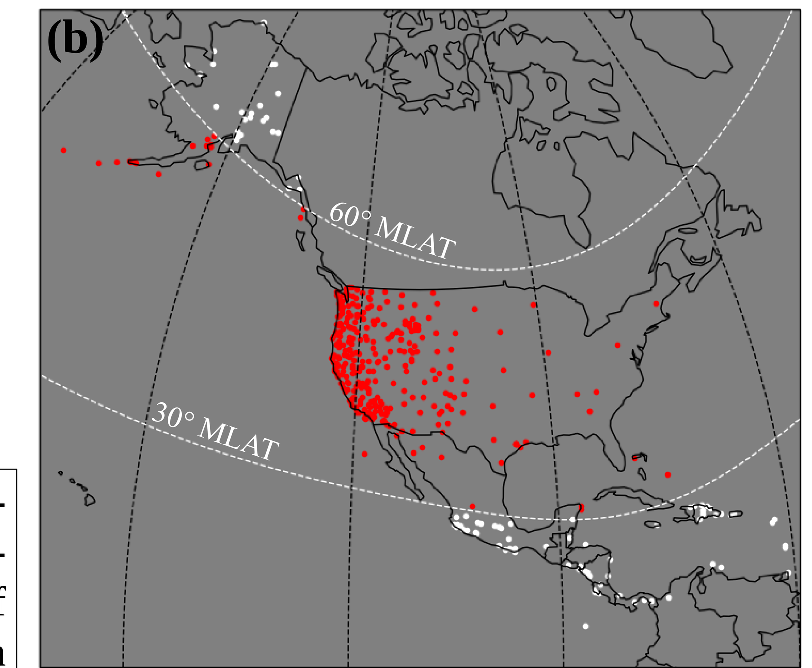

We present detailed observations of mid-latitude GPS scintillation for the green-shaded time frame in Figure 3. Statistics of scintillation strength and occurrence as a function of magnetic latitude are presented for 2 days (grey-shaded area)

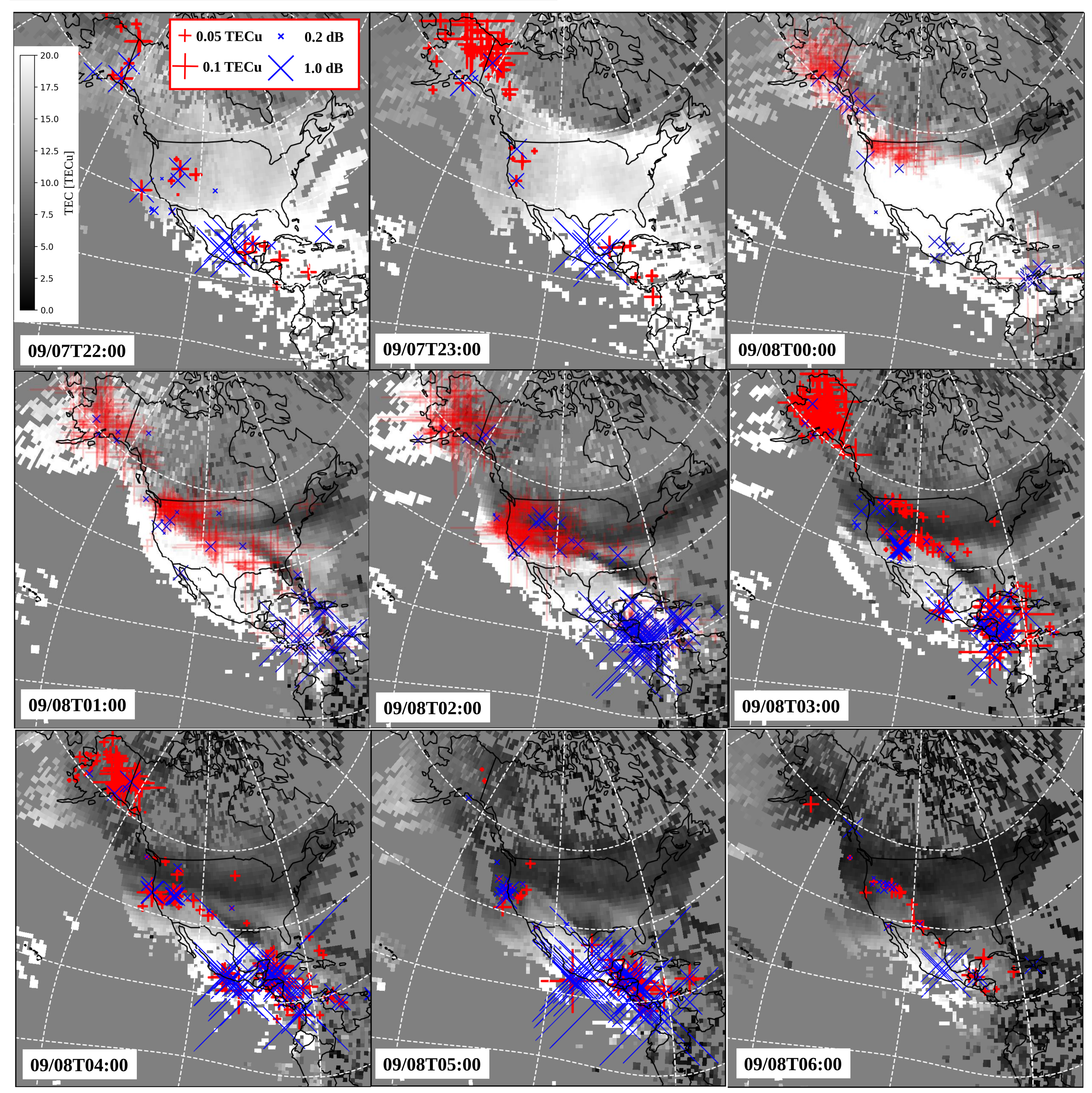

Figure 4: Hourly snapshots of scintillation strength and occurrence during the September 7-8 storm. Red pluses mark the phase/TEC scintillation, while blue crosses are amplitude/SNR scintillation.

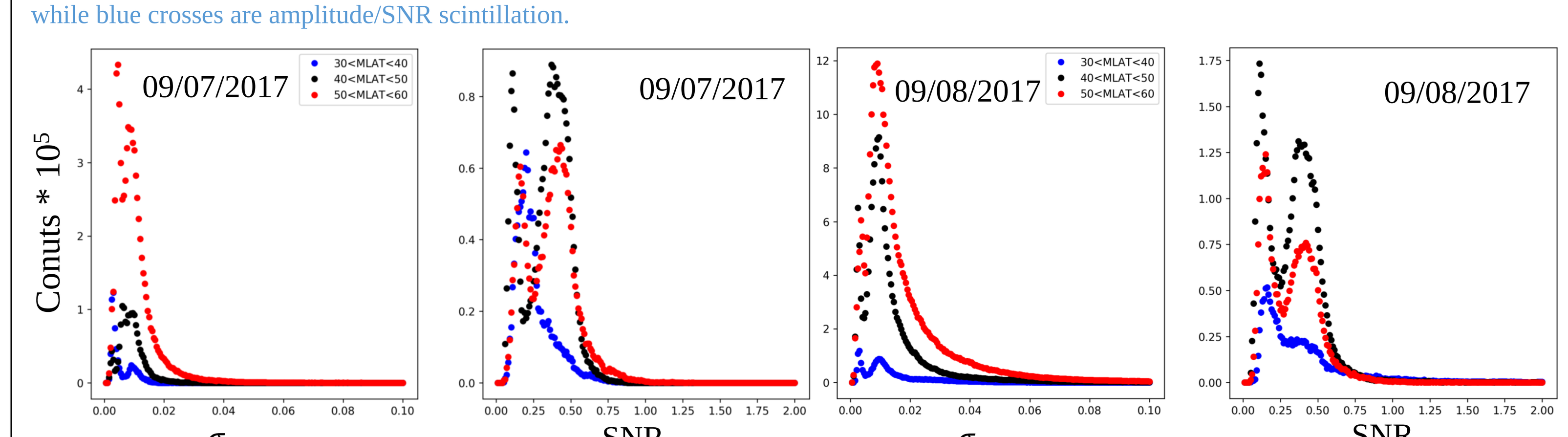

Figure 5: Statistics of strength vs. occurrence rate of scintillation per magnetic latitude bins. Statistics is from all receivers (~320) for a time period od a whole day, together covering the gray-shaded time-range from the Figure 3.

Validation: SWARM

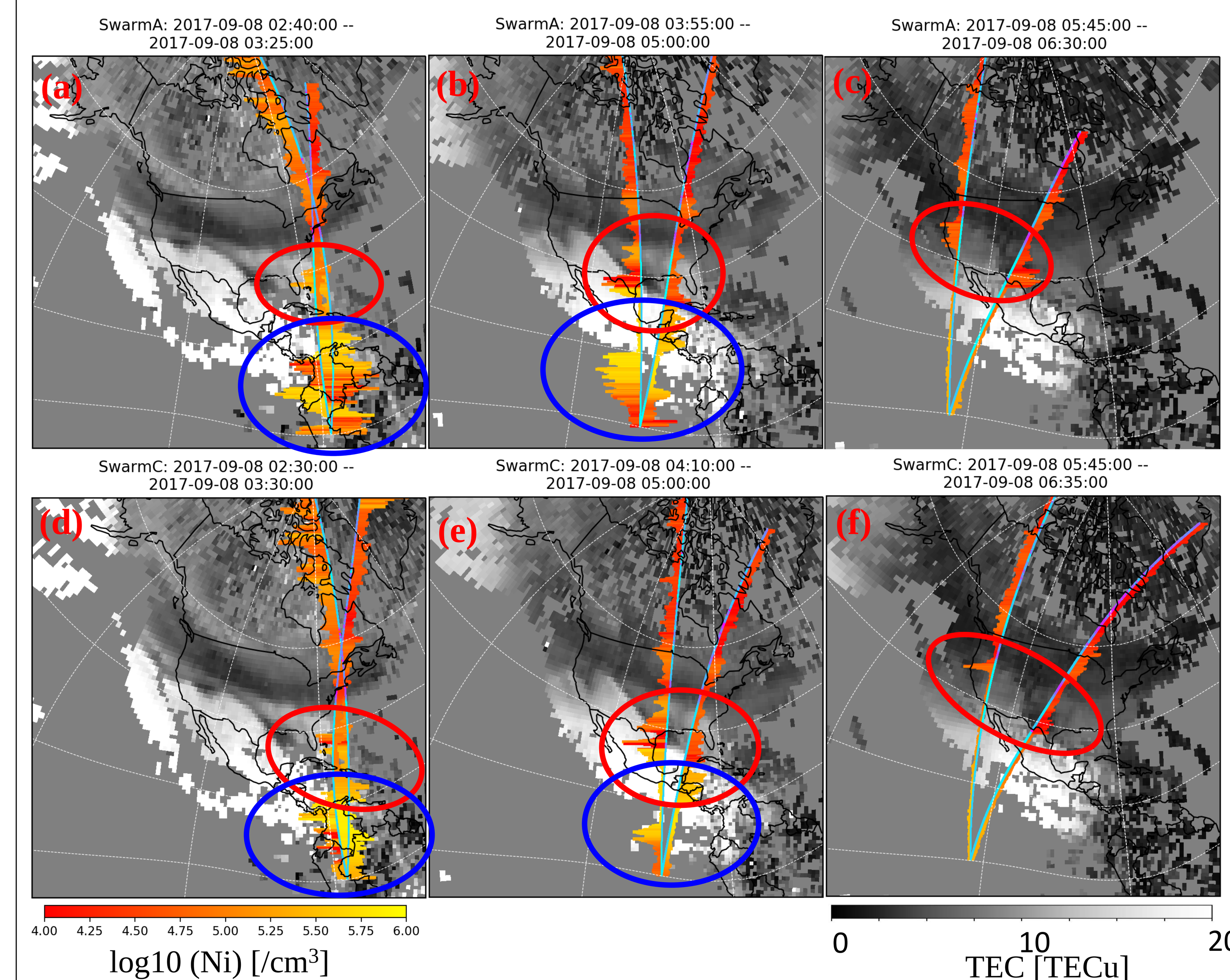

Figure 6: Snapshots of SWARM A and C satellite measurements of plasma density (Ni), density irregularities, and electron temperature. Each snapshot shows one satellite pass along magnetic-north foot point of trajectory. Background are GPSTEC maps. Locations of strong irregularities are highlighted with red (phase scintillation) and blue (amplitude scintillation) circles.

SWARM satellites measurements of high-resolution (16 Hz) electron density are used to validate maps of GPS scintillation. Figure 6 presents 3 passes of A, and C satellites that traversed the American sector. Satellite path is plotted as its magnetic-north trajectory footpoint. Color indicated total electron density, while the length (right-left) is an envelope of the high-pass filtered electron density.

We find a great spatiotemporal agreement between locations of, SWARM and GPS measurements. We highlight regions of dominant amplitude (blue) and phase (red) scintillation in figures 6 - 7 (a time-series plot from Figure 6a).

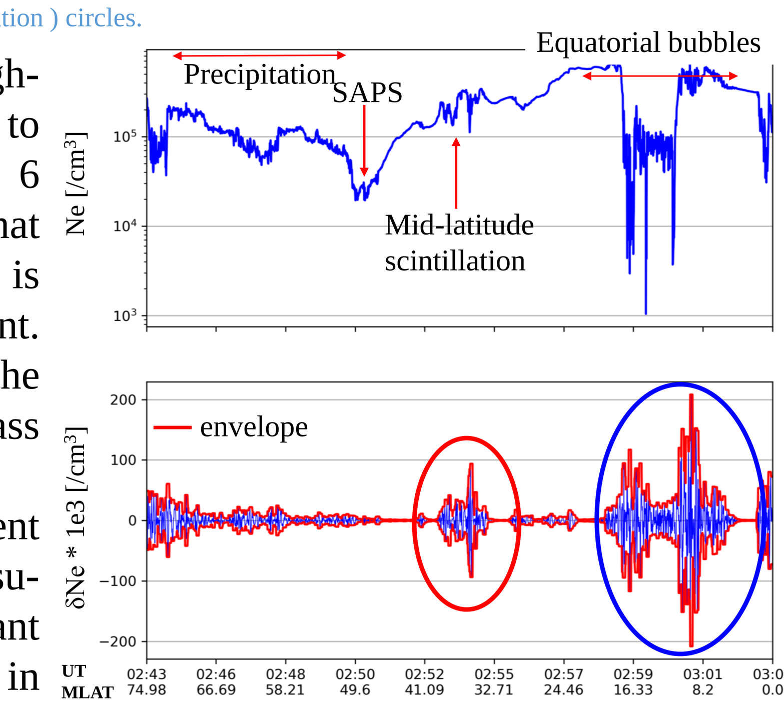

Figure 7:Time-series plot of electron density and de-trended density from the Figure 6a. Periods of intense phase (red) and amplitude (blue) scintillation from figure 6b are highlighted.

Conclusions

- First ever large-scale picture/observations of mid-latitude GPS scintillation is presented, utilizing the UNAVCO high-rate geodetic receivers.
- Receiver and time-dependent signal processing is introduced, as well as modified scintillation indices. Due to a large spread in receiver variance, the signal processing framework is receiver, and time dependent.
- **Observations taken during the 7-8 September 2017 geomagnetic storm show first the first large spread scintillation at mid-latitudes (Figure 4)!** Phase scintillation dominates in the earlier phase, while amplitude in the later phase of the storm. **Occurrence statistics in Figure 5 demonstrate that there are mid-latitude sources of amplitude scintillation.**
- In-situ measurements by the SWARM satellites show existence of kilometer-scale plasma irregularities, co-located with regions of strong GPS scintillation, providing an independent validation of physical implications of the measured scintillation occurrence.